Endocrine, *vol. 16, no. 1, 7–14, October 2001* 0969–711X/01/16:7–14/$12.00

The Endogenous Progesterone Metabolite, 5α-Pregnane-3,20-dione, Decreases Cell-Substrate Attachment, Adhesion Plaques, Vinculin Expression, and Polymerized F-actin in MCF-7 Breast Cancer Cells

John P. Wiebe and David Muzia

Hormonal Regulatory Mechanisms/Department of Zoology, University of Western Ontario, London, Ontario, Canada

Tumorous human breast tissue readily converts progesterone to 5α-pregnane-3,20-dione (5αP), and this metabolite has been shown to stimulate proliferation and to decrease adhesion of MCF-7 breast cancer cells. To determine the mechanisms of action of 5αP on cell adhesion, MCF-7 cells were grown without or with 5αP (10^{-9}–10^{-5} *M*), and the effects on cell and nuclear morphology, adhesion plaques, vinculin and actin expression, actin polymerization, and microfilament distribution were examined by immunohistochemistry, morphometry (using confocal microscopy and digital computer imaging analysis), and Western blotting. Treatment of cells with 10^{-9}–10^{-6} *M* 5αP resulted in dose-dependent decreases in cell area, cell-to-cell contacts, and attachment to the substratum, and increases in variation in nuclear area. These changes in the 5αP-treated cells were accompanied by decreases in vinculin-containing adhesion plaques, vinculin expression, polymerized actin stress fibers, and decreases in insoluble and increases in soluble actin fractions. The results suggest that the observed decreases in adhesion and increases in cell proliferation following 5αP treatment may be owing to depolymerization of actin and decreased expression of actin and vinculin. We conclude that the endogenous progesterone metabolite, 5αP, may be involved in promoting breast neoplasia and metastasis by affecting adhesion and cytoskeletal molecules.

Key Words: Progesterone metabolite; 5α-pregnane-3,20-dione; breast cancer; adhesion plaques; vinculin; actin.

Introduction

Progesterone is required for the full proliferative activity of human female breast tissue *(1,2)* and may be directly or indirectly involved in either stimulating or inhibiting breast cancer *(3,4)*. A number of studies have shown that progesterone, or various derivatives with progestational activities, may stimulate or inhibit tumor growth in vivo *(5–8)* and cell proliferation *(9,10)* and cell-cycle progression *(11)* in vitro. We have recently shown that stimulatory and inhibitory actions of progesterone might result from two different types of endogenous metabolites *(12)*. Evidence from tissue metabolism studies *(12)* shows that tumorous breast tissue converted progesterone into significantly greater amounts of 5α-pregnane steroids, particularly 5α-pregnane-3,20-dione (5αP), whereas normal (nontumorous) tissue from the same breast produced significantly more δ-4-pregnene steroids, especially 3α-hydroxy-4-pregnen-20-one (3αHP). The 5α-reduced steroids, such as 5αP stimulated, whereas 4-pregnenes such as 3αHP inhibited proliferation in several breast cell lines *(12)*. Additionally, 5αP enhanced detachment, whereas 3αHP increased attachment, of MCF-7 cells to the substratum. Other studies *(13)* have identified the presence of specific and separate high-affinity receptors for 5αP and 3αHP in the plasma membrane fraction of MCF-7 breast cancer cells and indicate that the receptor numbers may be modulated by exposure to estradiol *(13)*. These findings lend support for the potential regulatory role of progesterone metabolites in the development and metastasis of breast cancer.

Transformation of normal cells to cancerous cells is generally accompanied by alterations in cell and nuclear morphology *(14–18)*, organization of the actin cytoskeleton *(19–22)*, and cell-cell and cell-substrate adhesion *(23–25)*. Vinculin is a membrane-associated cytoskeletal protein localized at both the cell-to-cell and cell-to-substrate adhesive plaques *(26–28)*. In the polymerized form, it functions as a binding protein between the transmembrane proteins and actin fibers *(28)*. While vinculin is readily detected in normal cell lines, its organization may be greatly altered

Received July 30, 2001; Revised September 19, 2001; Accepted September 20, 2001.

Author to whom all correspondence and reprint requests should be addressed: Dr. John P. Wiebe, Hormonal Regulatory Mechanisms, B&G Building, Room 344, University of Western Ontario, London, Ontario N6A 5B7 Canada. E-mail: jwiebe@uwo.ca

Table 1
Effect of 5αP and 3αHP on Cell Detachment and Attachment[a]

		5αP			3αHP		
	Control	10^{-8} *M*	10^{-7} *M*	10^{-6} *M*	10^{-8} *M*	10^{-7} *M*	10^{-6} *M*
% Detached	46.8 ± 3.1	49.1 ± 2.9	63.6 ± 3.0[b]	67.0 ± 2.5[b]	42.9 ± 3.2	30.7 ± 3.1[c]	31.4 ± 3.3[b]
% Attached	57.5 ± 2.1	55.8 ± 2.2	41.7 ± 3.3[c]	34.1 ± 3.5[b]	58.2 ± 2.1	67.8 ± 2.0[b]	72.4 ± 2.2[b]

[a] The cellular detachment ($n = 4$) and attachment ($n = 3$) determinations were performed in separate experiments using the procedures described previously *(12)* following 72 h of culture in the presence of treatment media.
[b] $p < 0.01$.
[c] $p < 0.05$.

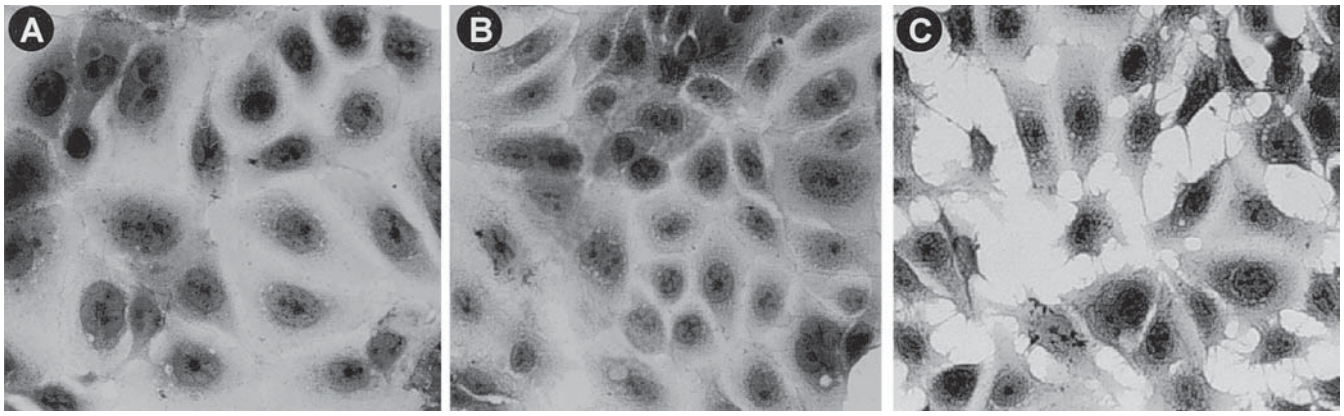

Fig. 1. Effect of 3αHP and 5αP on cellular morphology of subconfluent MCF-7 cells in culture. The control cells (**A**) and 3αHP-treated (**B**) cells show near continuous cell-cell contact, whereas the 5αP-treated cells (**C**) show marked cytoplasm withdrawal and discontinuous cell-cell contacts.

(29) or it may not be detected at all in highly malignant cell lines *(30)*, suggesting that depolymerization or suppression of vinculin may be closely related to malignant progression of cell systems.

Steroids have been shown to alter actin organization *(31,32)* and cellular adhesion *(33–37)*. Since 5αP and 3αHP have been shown to alter cell proliferation and adhesion *(12)*, the two cardinal aspects of cancer, our objective was to examine their effects on the actin cytoskeleton, on adhesion plaques and adhesion plaque–associated vinculin, and on general morphology of MCF-7 breast cancer cells in vitro. We report here the first evidence that exposure of MCF-7 cells to 5αP results in alteration in cell area and shape; increases in nuclear size variation; and significant decreases in cell-substrate attachment, polymerized F-actin, vinculin-associated adhesion plaques, and vinculin expression. Exposure to 3αHP did not result in significant changes from the controls. The results suggest that the endogenous progesterone metabolite, 5αP, may stimulate cell proliferation and detachment in part by affecting actin and vinculin expression and/or polymerization.

Results

Cellular Detachment/Attachment

Treatment of MCF-7 cells with 5αP at 10^{-7} and 10^{-6} *M* resulted in a significantly greater number of cells detached from, and significantly fewer cells attached to, the substrate (Table 1). Conversely, treatment with 3αHP at 10^{-7} and 10^{-6} *M* resulted in significantly fewer cells detached and more cells attached than controls (Table 1). These detachment/attachment results confirm previously published findings *(12)*.

Cell Morphology

Confluent untreated and control MCF-7 cells exhibited continuous contact with adjacent cells (Fig. 1A). Cells treated with 3αHP (Fig. 1B) did not show observable differences in morphology from controls. Treatment of cells with 10^{-6} *M* 5αP (Fig. 1C) resulted in retraction of the cellular cytoplasm, leaving behind lamelipodia-like and filopodia-like processes and resulting in discontinuous cell-to-cell contacts that were usually seen as point contacts via

Table 2
Effect of 5αP and 3αHP
on Cellular and Nuclear Area and Shape[a]

	Cell area (μm^2)	Cell shape index	Nuclear area (variation)
Control	545 ± 23	2.66 ± 0.21	24.28
5αP	401 ± 25[b]	3.43 ± 0.31[c]	68.57[d]
3αHP	556 ± 26	2.56 ± 0.2	22.57

[a] MCF-7 cells were treated with steroids at different concentrations (10^{-8}–10^{-6} *M*) for 72 h, and the effect on cell area, cell shape, and variation in nuclear area were determined as described in Materials and Methods. Only results from 10^{-6} *M* steroid concentrations are given.
[b] $p < 0.001$.
[c] $p < 0.05$.
[d] $p < 0.01$.

cellular microspikes or small filopodia-like structures. Treatment of cells with 5αP concentrations between 10^{-9} and 10^{-7} *M* resulted in an apparent dose-dependent decrease in retraction of the cytoplasm, with concentrations lower than 10^{-9} *M* showing no observable difference from controls.

Morphometric analyses (Table 2) showed that MCF-7 cells treated with 10^{-6} *M* 5αP had a significantly smaller cellular area, greater complexity of cell shape (cell shape index), and greater variance in nuclear size compared to controls or 3αHP-treated cells. Cells treated with 10^{-7} *M* 5αP showed intermediate effects, and cells treated with 5αP at concentrations $<10^{-7}$ *M* showed apparent (albeit statistically insignificant) dose-dependent effects on cellular area, cell shape index, and variance in nuclear area (results not shown).

Vinculin-Containing Adhesion Plaques

In control cells, vinculin-containing adhesion plaques appeared at the periphery and basally (Fig. 2A). Treatment of cells with 5αP resulted in marked loss in visualization of adhesion plaques (Fig. 2B). Analysis of cell adhesion plaque numbers showed that 5αP treatment resulted in a significant dose-dependent decrease (Fig. 2C) by as much as 75% at 10^{-6} and 10^{-5} *M*. Treatment with 3αHP did not result in significant changes in plaque numbers (Fig. 2C). Digital computer image system (DCIS) analysis showed a significant dose-dependent decrease in fluorescence of adhesion plaques in 5αP-treated cells (results not shown).

Vinculin expression as determined by Western blot analysis was prominent in control cells and was markedly decreased in cells treated with 10^{-6} *M* 5αP (Fig. 2D, inset). The suppression of vinculin expression was dose dependent between 10^{-9} and 10^{-6} *M* (Fig. 2D) with approx 75% reduction at 10^{-6} or 10^{-5} *M* 5αP. Treatment with 3αHP did not result in significant changes in vinculin expression (Fig. 2D).

Actin Cytoskeleton

Untreated (control) MCF-7 cells showed a ring of actin stress fibers running tangentially to one another (Fig. 3A), with a few fibers crossing the body of the cell (i.e., in a transcellular configuration). Stress fibers in the peripheral ring arrangement were generally bound to locations at the periphery of the cell. The transcellular fiber system, consisting of parallel fibers crossing the body of the cell, occurred more frequently in cells in subconfluent and confluent cultures than in cells growing in isolation. Treatment with 10^{-6} *M* 5αP resulted in almost complete loss of observable stress fibers (Fig. 3B). Quantitative analysis showed a significant dose-dependent decrease in actin stress fiber numbers (Fig. 3C) with approx 80% fewer stress fibers at 10^{-6} *M* than in control cells. Digital computer image analysis of phalloidin-rhodamine-stained stress fiber fluorescence confirmed the dose-dependent decrease (data not shown). Treatment with 3αHP did not result in significant changes in stress fiber number, although a trend toward an apparent increase was suggested (Fig. 3C).

The cellular concentrations of soluble (monomeric) and insoluble (polymeric) actin were studied by Western blotting. Extracts from control cells contained considerable amounts of insoluble F-actin and only small amounts of the soluble form (Fig. 3D, inset). Treatment of MCF-7 cells with 5αP resulted in increased concentrations of soluble and decreased concentrations of insoluble actin (Fig. 3D, inset). Quantitative analysis of the effects of various 5αP concentrations showed a dose-dependent increase in the ratio of soluble:insoluble actin (Fig. 3D). Treatment with 3αHP did not result in significant changes in the ratio of soluble:insoluble actin (Fig. 3D).

Discussion

Changes in cellular and nuclear size and shape have been used for some time in assessing alterations in cellular tumorigenicity and metastasis *(14–16)*. Cells treated with the progesterone metabolite, 5αP, displayed a dose-dependent decrease in cell area, increases in irregularity of cell shape, and increased variation in nuclear size, as determined by computerized morphometric image analysis. The results provide the first demonstration that a progesterone metabolite produced at relatively higher levels in tumorous than nontumorous breast tissue *(12)* can alter the morphology of breast cancer cells in vitro in a manner similar to that observed during neoplastic transformation of cells in vivo *(16,17,38–40)*.

The changes in morphology observed in cells undergoing neoplastic transformations that result in altered cell proliferation and acquisition of metastatic capacity have been shown to be accompanied by rearrangements of cytoskeletal and adhesion structures *(18–24,38,41,42)*. Cancerous cells possess a cytoskeleton that is organized differently

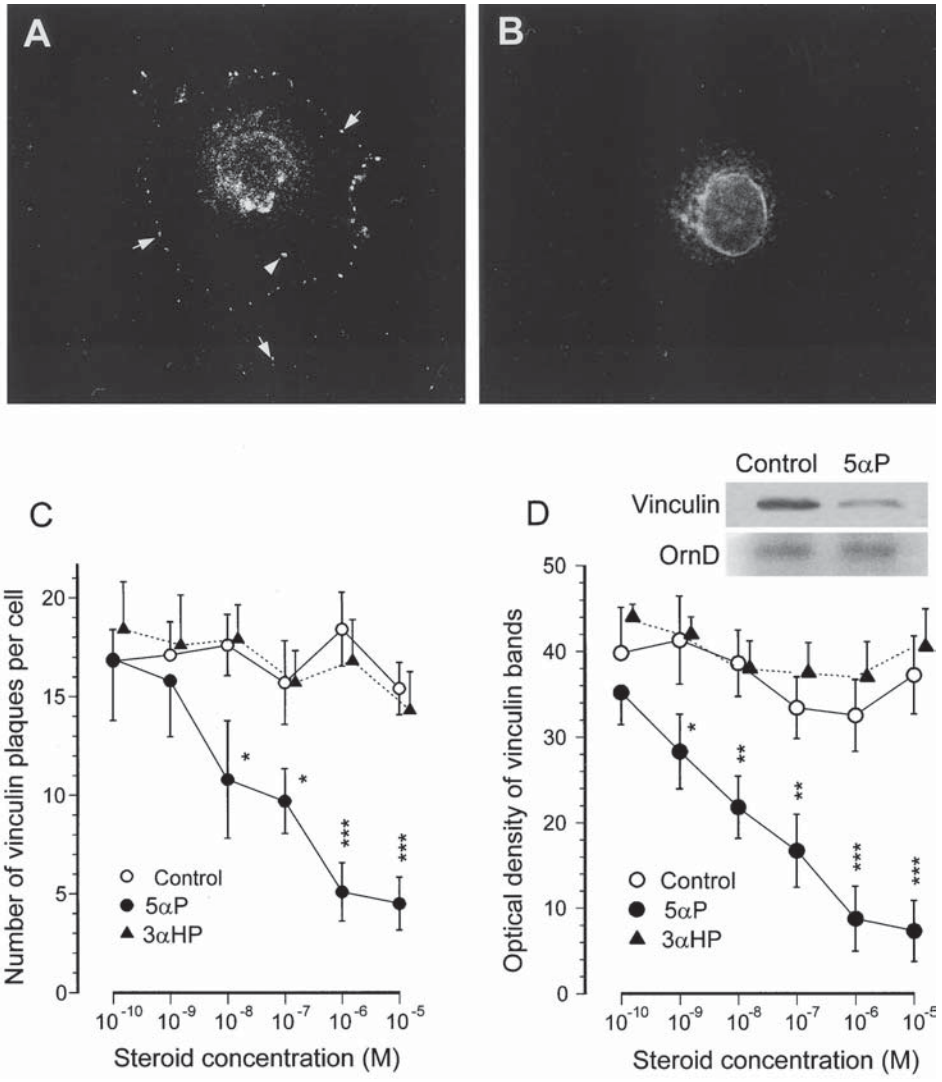

Fig. 2. Effect of 5αP on vinculin-containing adhesion plaques and vinculin expression in MCF-7 cells. (**A**) Control cells showing vinculin-containing plaques outlining the perimeter (arrows) and appearing basally (arrowhead). (**B**) 5αP-treated cells (10^{-6} *M*) showing only diffuse nuclear and perinuclear staining and absence of distinct peripheral and basal vinculin-containing plaques. The effects of treatment with 5αP (or 3αHP) on (**C**) number of vinculin-containing plaques and (**D**) vinculin expression are illustrated graphically. The inset in (**D**) shows typical Western blots for vinculin expression in control and 5αP-treated (10^{-6} *M*) cells as well as ornithine decarboxylase (OrnD) standard. *, **, and *** indicate significantly different from control at $p < 0.05$, $p < 0.01$, and $p < 0.001$, respectively.

from normal cells *(18–22)*, and highly metastatic cells possess a different cytoskeletal organization than low metastatic cells *(25,30)*. The greater level of organization of the actin cytoskeleton observed in normal cells *(42,43)* is characterized by higher levels of polymerized actin, whereas transformation to the metastatic condition may be accompanied by marked disruption and/or disappearance of actin filaments *(25)*. In the present study, treatment with 5αP resulted in a dose-dependent decrease in actin stress fiber number and the amount of polymerized actin. These results are in agreement with previous studies showing that the degree of polymerization of the actin cytoskeleton decreases in cells stimulated to higher rates of proliferation and with the acquisition of metastatic capacity *(19,22,25)*.

Cellular adhesion is a critical aspect of cancer biology. Changes in adhesion must take place when cells detach from the site of the original tumor, and when they metastasize to a new site. Therefore, changes in cell adhesive properties might be considered a primary factor leading to metastasis and, ultimately, malignancy *(24)*. Cells adhere to the substrate and to other cells via cell-cell and cell-substrate adhesion plaques. Cell-cell focal adhesion plaques contain cadherins, while cell-substrate adhesion plaques contain integrins *(28)*. In MCF-7 cells, vinculin is present at the integrin-mediated cell-substrate adhesion sites, whereas at the cadherin-mediated cell-cell adhesion sites, it is α-catenin that binds the ends of actin filaments to the cadherin complex *(44)*. Treatment of MCF-7 cells with 5αP resulted in a significant

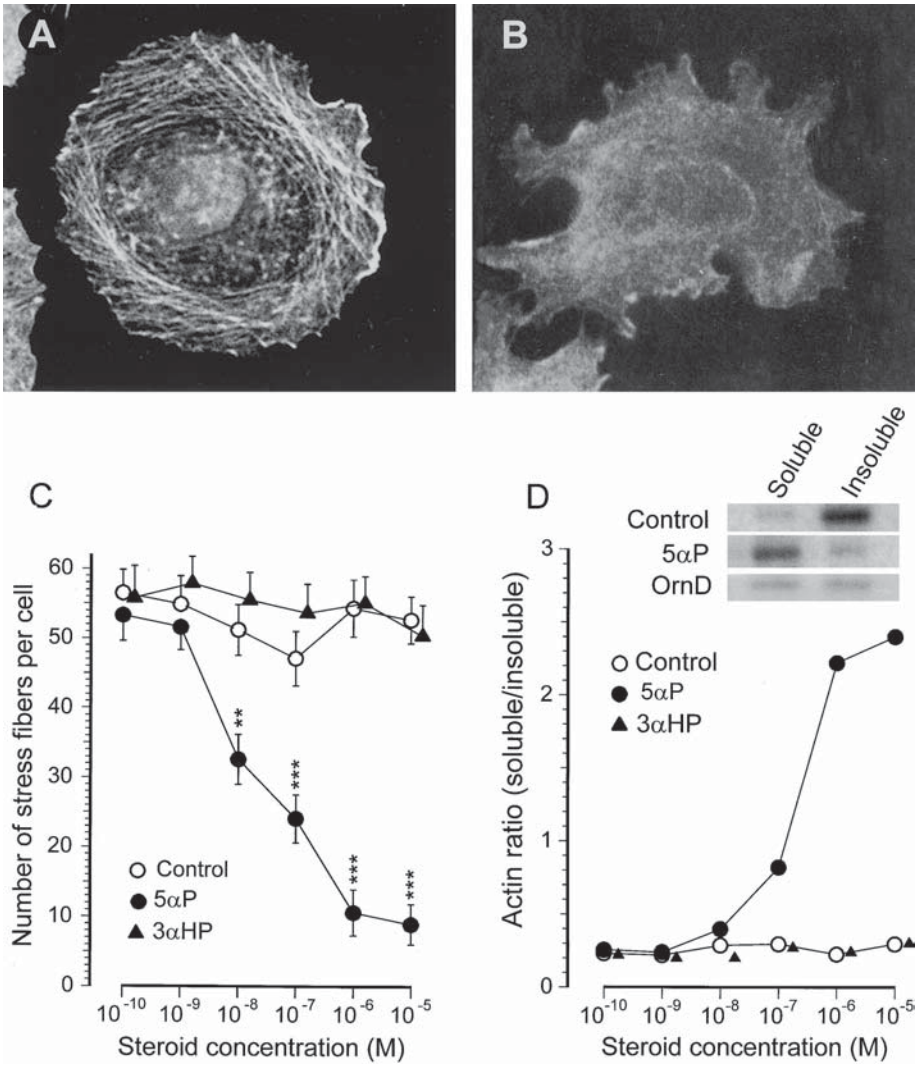

Fig. 3. Effect of 5αP on actin stress fibers in MCF-7 cells. (**A**) Control cells showing many actin stress fibers running tangentially to one another and bound to locations at the periphery. (**B**) Treatment with 10^{-6} *M* 5αP showing marked loss of observable actin fibers. The effects of treatment with 5αP (and 3αHP) on (**C**) number of actin stress fibers and (**D**) change in concentrations of soluble and insoluble actin are illustrated graphically. The inset in (**D**) shows representative Western blots of soluble and insoluble actin fractions from control and 5αP-treated (10^{-6} *M*) cells as well as ornithine decarboxylase (OrnD) standard. ** and *** indicate significantly different from control at $p < 0.01$ and $p < 0.001$, respectively.

dose-dependent reduction in the total number of vinculin-containing adhesion plaques and in vinculin expression. These decreases coincided with the observed dose-dependent decreases in cell adhesion. Our findings agree with other studies that have demonstrated coincidence between increased cellular proliferation or metastatic ability and decreased cellular adhesion, vinculin-containing adhesion plaques, and vinculin expression *(25,31,34,46)*. Treatment of cells with estrogen *(47)*, progesterone *(48)*, and glucocorticoids *(35,36)* has been shown to result in a decrease in adhesion to the substrate and to other cells. Our results therefore suggest that the endogenous progesterone metabolite, 5αP, may cause decreased adhesion by interfering with vinculin expression and reducing adhesion plaque numbers.

Treatment of MCF-7 cells with 3αHP resulted in decreased cell proliferation and increased cell adhesion *(12)*. This agrees with studies that show increased adhesion in cells that have a decreased rate of proliferation *(31,37)*. Although increased adhesion resulted from 3αHP treatment, the number and size of vinculin-containing adhesion plaques and the expression of vinculin were not significantly altered. One possible explanation may be that not all the adhesion plaques in MCF-7 cells use vinculin as a binding protein *(44)*. At the cell-cell adhesion sites, α-catenin binds competitively to cadherin complexes, outcompeting vinculin for cadherin binding *(44)*. In the absence of α-catenin, vinculin will bind to the cadherin complex, theoretically assuming the same role. Since MCF-7 cells express both vinculin and

α-catenin, it is possible that 3αHP treatment of MCF-7 cells resulted in an alteration in the number of α-catenin-containing cell-cell adhesion sites. An increase in the number of these cell-cell adhesion sites, in turn, would be expected to increase adhesion of the cell, without affecting the number or size of vinculin-containing adhesion plaques. In our studies, α-catenin was not explored, and the potential role of 3αHP on this adhesion site protein remains to be investigated.

In conclusion, our study shows that the progesterone metabolite, 5αP, which has been shown to be produced in greater amounts by tumorous than nontumorous breast tissue, significantly alters the morphology, decreasing actin polymerization, adhesion plaques, and vinculin expression. These changes are similar to those reported for cells showing neoplastic and metastatic transformations and may explain the observed increases in proliferation and detachment resulting from exposure to 5αP. The evidence is consistent with the hypothesis that progesterone metabolites (such as 5αP) found endogenously in human breast tissue may be involved in promoting breast tumor neoplasia and malignancy.

Materials and Methods

Chemicals

3αHP was synthesized and purified as previously described *(48)*. 5αP, progesterone, Dulbecco's Minimal Essential Medium:F12-Ham (DMEM), penicillin, streptomycin, insulin, trypsin, EDTA, Dextran T-70, phalloidin-TRITC, Triton X-100, bovine serum albumin (BSA), mouse monoclonal antivinculin and antiactin antibodies, mouse antiornithine decarboxylase and goat antimouse IgG-AP antibodies, dithiothreitol (DTT), phenylmethylsulfonyl fluoride (PMSF), bacitracin, leupeptin, and Tris-HCl were obtained from Sigma (Oakville, Ontario). Calf serum and fungizone were from Gibco-BRL (Burlington, Ontario).

Cell Culture

MCF-7 human breast adenocarcinoma cells were obtained from the Barbara Ann Karmanos Cancer Institute (Detroit, MI) at passage 134. The cells were grown in DMEM:F12 Ham in a 1:1 ratio. The culture medium was supplemented with 5% calf serum, penicillin (100 U/mL), streptomycin (100 μg/mL), fungizone, insulin (10 μg/mL), and sodium bicarbonate (1.2 mg/mL). The cells designated for experimental use were grown in culture medium containing serum that had been stripped with dextran-coated charcoal to remove steroids. The cells were grown and passaged in T-75 flasks maintained in a humidified incubator at 37ºC, with a 5% CO_2 atmosphere. Cells were harvested at approx 80% confluence using 0.1% trypsin and 0.05% EDTA in phosphate-buffered saline (PBS) (pH 7.2). Cell viability was determined by Trypan blue exclusion.

Cell Attachment or Detachment

Cell attachment and detachment was determined as described previously *(12)*.

Cell Morphology and Immunohistochemistry

Cells were seeded onto acid-washed glass cover slips (22 × 22 mm) held in 35-mm plastic Petri dishes and were cultured for 72 h in experimental media, either without added steroids (controls) or containing appropriate concentrations of 5αP or 3αHP. Media were changed every 24 h.

Morphology and Morphometry

After the treatment period, cells were fixed in 2% formaldehyde:PBS and then stained with either Ehrlich's hematoxylin and eosin (for general morphology and nuclear area and shape) or Giemsa stain (for cell area and cell shape). Cell and nuclear areas were calculated using DCIS (Northern Exposure Image Analysis Software, Empix Imaging, Mississauga, Ontario) calibrated to a ×40 objective and based on area/pixel value. The DCIS determined the total number of pixels within the cross-sectional area of a scanned cell or nucleus and the total number of pixels comprising the perimeter of the object. About 250 cells and nuclei per treatment (from 10 replicate cover slips) appearing on a transverse grid were selected from separate ocular fields. The cell shape index was calculated by the DCIS using the following formula *(49)*:

$$\text{Cell shape} = \frac{(\text{Perimeter})^2}{4\pi \cdot \text{Area}}$$

Actin Stress Fibers

After the treatment period (usually 72 h), cells were rinsed for 10 min in two changes of PBS and fixed for 7–15 min in 2% formaldehyde:PBS at 37ºC, rinsed in two 10-min washes in PBS (room temperature), treated for 5 min with 0.1% Triton X-100, and then rinsed in three 5-min washes of PBS. To visualize actin stress fibers, the cells were stained in Phalloidin-TRITC (0.05 mg/mL of PBS) for 25 min at 4ºC in a humidity chamber.

Vinculin

For vinculin localization, cover slips were blocked for 15 min with 1% BSA (in PBS), incubated for 1 h with mouse monoclonal antivinculin antibody (diluted 1:50 in blocking buffer), and then for 1 h with secondary goat antimouse IgG-antibody conjugated to Phalloidin-TRITC (diluted 1:25 with PBS). Following the incubations, all cover slips were rinsed in three 5-min washes of PBS and mounted on glass slides using glycerol:PBS (9:1, pH 9.0). Cells were examined with a Bio-Rad MRC-600 Laser Scanning Confocal Microscope.

Quantitation of Numbers of Stress Fibers and Adhesion Plaques

Cells were magnified until they filled the field of view. Stress fibers were counted if they were linear, well defined within the cell, and if both ends of a filament were visible. Vinculin-stained adhesion plaques were counted (45 cells per treatment in each experiment; 10 experiments). Fluorescence brightness of stress fibers and adhesion plaques in rhodamine-stained cells was analyzed by DCIS using confocal image analysis *(50)*. The DCIS program was calibrated to the ×40 objective lens to determine both the total number of pixels per cell and the optical gray scale of each individual pixel. The average optical gray scale per pixel was calculated for each scanned cell, and this value was used to represent the average brightness of fluorescence in a cell. Greater fluorescence indicated larger amounts of polymerized actin or vinculin within a cell. Within each treatment group, separate cover slips were used to determine background staining. Background controls for actin were treated with 10^{-6} *M* cytochalasin D for 10 min (to depolymerize stress fibers) before staining with phalloidin-rhodamine. Background controls for vinculin were treated only with goat antimouse IgG secondary antibody in the absence of primary treatment with antivinculin antibody. The average optical intensity gray scale per pixel was calculated for each scanned background control cell, and this value was subtracted from the average intensity of experimentally treated cells to determine fluorescence owing to specific actin and vinculin staining, respectively.

Actin and Vinculin Expression

Cells were cultured in T-75 plastic culture flasks for 72 h, to approx 80% confluence, in experimental media containing either no additional hormones (control) or various concentrations of 5αP or 3αHP. Media were removed and 500 µL/flask of lysis buffer (50 m*M* Tris-HCl, 100 m*M* DTT, 2% sodium dodecyl sulfate [SDS], 10% glycerol, 1 m*M* PMSF, and 0.1% bromophenol blue) was added. The cell lysate was collected, boiled for 10 min, repeatedly passed through a 21-gage needle, and centrifuged at 10,000*g*, and the supernatant was used in the SDS-polyacrylamide gel electrophoresis.

Isolation of Soluble and Insoluble Actin

MCF-7 cells were lysed with Triton solution (2% Triton X-100; 160 m*M* KCl; 40 m*M* imidazole-HCl; 20 m*M* EGTA; 8 m*M* sodium azide, pH 7.0) for 10 min at 0ºC and centrifuged at 10,000*g* for 10 min. The supernatant (1 mL) was mixed with running buffer (300 µL) and boiled for 5 min to obtain the soluble actin (G-actin) fraction. The pellets were dissolved in lysis buffer, incubated in a boiling water bath for 10 min, and vortexed vigorously for 1 min to obtain the insoluble actin (F-actin).

Western Blotting

Cytoskeletal proteins were transferred to a nitrocellulose membrane (Bio-Rad) overnight at 4ºC. After transfer, the nitrocellulose membranes were blocked for 1 h in blocking buffer (1% BSA in PBS). Nitrocellulose blots were then incubated with either primary antiactin antibody at a 1:100 dilution or primary antivinculin antibody at a 1:40 dilution in blocking buffer for 2 h at 4ºC with gentle agitation. After incubation, the nitrocellulose blots were washed with three 10-min rinses of blocking buffer and transferred to a solution of secondary goat antimouse IgG conjugated to alkaline phosphatase at a dilution of 1:2000 in blocking buffer. Western blotting for ornithine decarboxylase was similar to that of actin and vinculin except that the nitrocellulose membranes were incubated with antiornithine decarboxylase antibody at a 1:80 dilution in blocking buffer. All Western blots were developed with a goat antimouse alkaline phosphatase Western blot visual detection kit. The blots were scanned and images analyzed by digitizing software (Un-Scan-It gel for Windows; Silk Scientific). Protein concentrations were determined by the Bradford *(51)* method.

Acknowledgments

This work received financial support from Canadian Breast Cancer Research Initiative Grant 007166, NSERC Grant A6865, and the Komen Breast Cancer Foundation.

References

1. Going, J. J., Anderson, T.J., Battersby, S., and MacIntyre, C. C. A. (1988). *Am. J. Pathol.* **130,** 193–204.
2. Potten, C. S., Watson, R. J., Williams, G. T., Tickle, S., Roberts, S. A., Harris, M., and Howel, A. (1988). *Br. J. Cancer* **58,** 163–170.
3. Pike, M. C., Spicer, D. V., Dahmoush, L., and Press, M. F. (1993). *Epidemiol. Rev.* **15,** 17–35.
4. King, R. J. B. (1991). *J. Steroid Biochem. Mol. Biol.* **39,** 811–818.
5. Santen, R. J., Manni, A., Harvey, H., and Redmond, C. (1990). *Endocr. Rev.* **11,** 221–265.
6. Anderson, T. J., Battersby, S., King, R. J. B., McPherson, K., and Going, J. J. (1989). *Hum. Pathol.* **20,** 1139–1144.
7. Groshong, S. D., Owen, G. I., Grimison, B., Schauer, I. E., Todd, M. C., Langan, T. A., Sclafani, R. A., Lange, C. A., and Horwitz, K. B. (1997). *Mol. Endocrinol.* **11,** 1593–1607.
8. Braunsberg, H., Coldham, N. G., Leake, R. E., Cowan, S. K., and Wong, W. R. (1987). *Eur. J. Cancer Clin. Oncol.* **23,** 563–572.
9. Clark, C. L. and Sutherland, R. L. (1990). *Endocr. Rev.* **11,** 266–302.
10. Cappelletti, V., Miodini, P., Fioravanti, L., and Di Fronzo, G. (1995). *Anticancer Res.* **15,** 2551–2556.
11. Musgrove, E. A. and Sutherland, R. L. (1994). *Semin. Cancer Biol.* **5,** 381–389.
12. Wiebe, J. P., Muzia, D., Hu, J., Szwajcer, D., Hill, S. A., and Seachrist, J. L. (2000). *Cancer Res.* **60,** 936–943.
13. Weiler, P. J. and Wiebe, J. P. (2000). *Biochem. Biophys. Res. Commun.* **272,** 731–737.
14. Fox, C. H., Caspersson, T., Kudynowski, J., Sanford, K. K., and Tarone, R. E. (1977). *Cancer Res.* **37,** 892–897.

15. Folkman, J. and Moscona, A. (1978). *Nature* **273,** 345–349.
16. Baak, J. P., Van Dop, H., and Kurver, P. H. (1985). *Cancer* **56,** 374–382.
17. Iwig, M., Czeslick, E., Muller, A., Gruner, M., Spindler, M., and Glaesser, D. (1995). *Eur. J. Cell Biol.* **67,** 145–157.
18. Dewhurst, L. O., Rennie, I. G., and MacNeil, S. (1998). *Melanoma Res.* **8,** 303–311.
19. Ben-Ze'ev, A. (1985). *Biochim. Biophys. Acta* **780,** 197–212.
20. Holme, T. C. (1990). *Eur. J. Surg. Oncol.* **16,** 161–169.
21. Lin, Z. X. (1993). *Chin. J. Oncol.* **15,** 8–11.
22. Holth, L. T., Chadee, D. N., Spencer, V. A., Samuel, S. K., Safneck, J. R., and Davie, J. R. (1998). *Int. J. Oncol.* **13,** 827–837.
23. Burridge, K. (1986). *Cancer Rev.* **4,** 18–78.
24. Raz, A. (1988). *Ciba Found. Symp.* **141,** 109–122.
25. Suzuki, H., Nagata, H., Shimada, Y., and Konno, A. (1998). *Int. J. Oncol.* **12,** 1079–1084.
26. Wilkins, J. A. and Lin, S. (1982). *Cell* **28,** 83–90.
27. Luna, E. J. and Hitt, A. L. (1992). *Science* **258,** 955–964.
28. Humphries, M. J. and Newham, P. (1998). *Trends Cell Biol.* **8,** 78–83.
29. Schliwa, M., Nakamura, T., Porter, K. R., and Euteneuer, V. (1984). *J. Cell Biol.* **99,** 1045–1059.
30. Sadano, H., Inoue, M., and Taniguchi, S. (1992). *Jap. J. Cancer Res.* **83,** 625–630.
31. Sapino, A., Pietribiasi, F., Bussolati, G., and Marchisio, P. C. (1986). *Cancer Res.* **46,** 2526–2531.
32. Koukouritaki, S. B., Margoris, A. N., Gravanis, A., Hartig, R., and Stournaras, C. (1997). *J. Cell. Biochem.* **65,** 492–500.
33. McCrohon, J. A., Jessup, W., Handelsman, D. J., and Celermajer, D. S. (1999). *Circulation* **99,** 2317–2322.
34. DePasquale, J. A., Samsonoff, W. A., and Gierthy, J. F. (1994). *J. Cell Sci.* **107,** 1241–1254.
35. Gronowicz, G. A. and McCarthy, M. B. (1995). *Endocrinology* **136,** 598–608.
36. Pearson, D. and Sheldon, P. (1995). *Adv. Exp. Med. Biol.* **371,** 167–170.
37. Lin, V. C., Ng, E. H., Aw, S. E., Tan, M. G., Ng, E. H., and Bay, B. H. (2000). *Mol. Endocrinol.* **14,** 348–358.
38. Baak, J. P., Kurver, P. H., De Snoo-Niewlaat, A. J., De Graef, S., Makkink, B., and Boon, M. E. (1982). *Histopathology* **6,** 327–339.
39. Wittekind, C. and Schulte, E. (1987). *Ann. Quant. Cytol. Histol.* **9,** 480–484.
40. Wolberg, W. H., Street, W. N., and Magasarian, O. L. (1997). *Cancer* **81,** 172–179.
41. Pokorna, E., Jordan, P. W., O'Neill, C. H., Zicha, D., Gilbert, C. S., and Vesely, P. (1994). *Cell Motil. Cytoskel.* **28,** 25–33.
42. Helige, C., Zellnig, G., Hoffman-Wellenhof, R., Fink-Puches, R., Smolle, J., and Tritthart, H. A. (1997). *Invas. Metast.* **17,** 26–41.
43. Bershadsky, A. D., Gluck, U., Denisenko, O. N., Sklyarova, T. V., Spector, I., and Ben-Ze'ev, A. (1995). *J. Cell Sci.* **180,** 1183–1193.
44. Hazan, R. B., Kang, L., Roe, S., Borgen, P. I., and Rimm, D. L. (1997). *J. Biol. Chem.* **272,** 32,448–32,453.
45. Berx, G., Nollet, F., and van Roy, F. (1998). *Cell Adhes. Commun.* **6,** 171–184.
46. Fujimoto, J., Ichigo, S., Hori, M., Morishita, S., and Tamaya, T. (1996). *J. Steroid Biochem. Mol. Biol.* **57,** 275–282.
47. Shi, Y. E., Liu, Y. E., Lippman, M. E., and Dickson, R. B. (1994). *Hum. Reprod.* **9(Suppl. 1),** 162–173.
48. Wiebe, J. P., Deline, C., Buckingham, K. D., Dave, V., and Stothers, J. B. (1985). *Steroids* **45,** 39–51.
49. Marchevsky, A. M. and Erler, B. S. (1994). In: *Image analysis: a primer for pathologists.* Marchevsky. A. M. and Bartels, P. H. (eds.). Raven Press, New York, pp. 125–180.
50. Usson, Y., Guignandon, A., Laroche, N., Lafage-Proust, M. H., and Vico, L. (1997). *Cytometry* **28,** 298–304.
51. Bradford, M. M. (1976). *Anal. Biochem.* **72,** 248–259.